

Crystal Structure of Human Frataxin*

Received for publication, June 26, 2000, and in revised form,
July 13, 2000
Published, JBC Papers in Press, July 18, 2000,
DOI 10.1074/jbc.C000407200

Sirano Dhe-Paganon‡, Ron Shigeta§,
Young-In Chi¶, Michael Ristow||**,
and Steven E. Shoelson‡‡

From the Joslin Diabetes Center and Department of
Medicine, Harvard Medical School, Boston,
Massachusetts 02215 and the ||Department of Internal
Medicine 2, University of Cologne, Cologne 50931,
Germany

Friedreich's ataxia, an autosomal recessive neurodegenerative disorder characterized by progressive gait and limb ataxia, cardiomyopathy, and diabetes mellitus, is caused by decreased frataxin production or function. The structure of human frataxin, which we have determined at 1.8-Å resolution, reveals a novel protein fold. A five-stranded, antiparallel β sheet provides a flat platform, which supports a pair of parallel α helices, to form a compact $\alpha\beta$ sandwich. A cluster of 12 acidic residues from the first helix and the first strand of the large sheet form a contiguous anionic surface on the protein. The overall protein structure and the anionic patch are conserved in eukaryotes, including animals, plants, and yeast, and in prokaryotes. Additional conserved residues create an extended 1008-Å² patch on a distinct surface of the protein. Side chains of disease-associated mutations either contribute to the anionic patch, help create the second conserved surface, or point toward frataxin's hydrophobic core. These structural findings predict potential modes of protein-protein and protein-iron binding.

Human genome sequencing initiatives promise to identify ever increasing numbers of disease-related genes, but finding a specific disease locus may not help to explain the encoded protein's function or why altered function causes disease. Friedreich's ataxia (1), the most common of the hereditary ataxias, is an example of this problem. Friedreich's ataxia is an auto-

somal recessive neurodegenerative disorder characterized clinically by the onset in the first two decades of life of limb ataxia, cerebellar dysarthria, skeletal deformities, and hypertrophic cardiomyopathy (1, 2). An increased incidence of blindness, deafness, impaired glucose tolerance, and diabetes mellitus indicate that this is a systemic disorder. The disease is invariably fatal due to its relentless progression. The *FRDA* disease locus on chromosome 9 (3) encodes the frataxin protein (4). Most patients are homozygous for a GAA trinucleotide repeat expansion in the first intron (4), which causes the DNA to be sticky (5) and leads to decreased transcription and diminished protein production (6). Fewer patients have a point mutation in one allele and an increase in GAA repeats in the other allele (7), confirming that Friedreich's ataxia is due to loss of function.

In eukaryotes frataxin is necessary for normal mitochondrial function (8, 9). Yeast strains lacking the homologue, Yfh1p, have defective mitochondrial respiration (9) and loss of mtDNA (8), and they accumulate iron in their mitochondria (10). Findings in mammalian cells (11) and human tissues (1, 12–14) suggest related problems when frataxin function is reduced, but because many genotypes lead to similar "sick mitochondria" phenotypes (15), no specific biochemical function for frataxin has been deduced. Nevertheless, its conservation in prokaryotes and eukaryotes, its importance in mitochondrial energy production, and the accumulation of iron in its absence suggest fundamental requirements in iron metabolism.

Eukaryotic frataxin homologues are expressed in the cytoplasm as larger precursors that are cleaved upon entry into mitochondria to yield mature proteins (16–19). In yeast, Yfh1p is cleaved by the mitochondrial processing protease to yield the mature, 122-amino acid active protein. Mature Yfh1p migrates on SDS-polyacrylamide gel electrophoresis as though it were a 21-kDa protein (17, 19). Human frataxin is similarly processed to an apparent 18-kDa protein, although precise sites of cleavage have not been reported. Bacterial frataxins naturally lack the mitochondrial localization signal altogether. The cleaved, mitochondrial localization signals are not conserved. In contrast, there is high homology among the mature yeast protein, the corresponding regions of other eukaryotic frataxins, and the encoded proteins from bacteria (Fig. 1). We have determined the x-ray crystal structure of mature human frataxin to predict potential functions and to provide a framework for testing hypotheses.

MATERIALS AND METHODS

Sample Preparation—A fragment of the frataxin gene corresponding to residues 88–210 of human frataxin was subcloned into a pET28a vector. A K135M mutation was created by site-directed mutagenesis using the polymerase chain reaction. Protein was expressed in *Escherichia coli* (BL21DE3) and purified using cobalt affinity medium. The His tag was cleaved using bovine thrombin (4 units/mg, 20 °C, 16 h), and the protein was further purified by anion-exchange chromatography (Mono-Q FPLC). Crystals were obtained at room temperature by equilibrating 1- μ l drops of 50 mg/ml protein in 5 mM Tris, pH 8.0, 0.3 M NaCl, 10 mM dithiothreitol and 1 μ l of crystallization buffer (2.5 M ammonium sulfate, 2% sucrose, 100 mM sodium citrate, pH 6.0) using the hanging drop method. Under identical crystallization conditions, crystals grew in two space groups ($P2_12_12_1$ and $C2$) within 7 days to $\sim 0.5 \times 0.5 \times 1.0$ mm. For the preparation of derivatives, the crystals were first equilibrated in stabilization buffer: 50 mM Hepes, pH 7.4, 3.8 M ammonium sulfate.

Data Collection—Native and derivative data sets were acquired at room temperature. All data sets were integrated and scaled with the DENZO/SCALEPACK (20) software package and merged using pro-

* This work was supported in part by National Institutes of Health Grant DK43123 (to S. E. S.). The costs of publication of this article were defrayed in part by the payment of page charges. This article must therefore be hereby marked "advertisement" in accordance with 18 U.S.C. Section 1734 solely to indicate this fact.

The atomic coordinates and structure factors (code 1EKG) have been deposited in the Protein Data Bank, Research Collaboratory for Structural Bioinformatics, Rutgers University, New Brunswick, NJ (<http://www.rcsb.org/>).

‡ Supported by an Iacocca Fellowship of the Joslin Diabetes Center.

§ Supported by National Institutes of Health Training Grant DK07260.

¶ Supported by a fellowship from the Juvenile Diabetes Foundation.

** Supported by a Koeln Fortune fellowship of the University of Cologne.

‡‡ Recipient of a Burroughs Wellcome Fund Scholar Award in Experimental Therapeutics. To whom correspondence should be addressed: Joslin Diabetes Center, One Joslin Place, Boston, MA 02215. Tel.: 617-732-2528; Fax: 617-735-1970; E-mail: Steven.Shoelson@Joslin.Harvard.edu.

TABLE I
Diffraction data

Statistics for the highest resolution bin are given in parentheses. Unit cell for P2₁2₁2₁ crystal form: $a = 43.96 \text{ \AA}$, $b = 45.13 \text{ \AA}$, $c = 68.94 \text{ \AA}$. Unit cell for C2 crystal form: $a = 87.53 \text{ \AA}$, $b = 32.64 \text{ \AA}$, $c = 93.73 \text{ \AA}$, $\beta = 90.67^\circ$. Derivative preparation conditions: Pt(NH₄)₂Cl₂, 0.5 mM soak overnight; K₂PtCl₆-1, 10 mM K₂PtCl₆ for 7 h; K₂PtCl₆-2, 8 mM K₂PtCl₆ for 12 h. Iodine: 1 mM chloramine T and 1 mM KI soak for 3.5 h.

Crystal/derivative	Native	Pt(NH ₄) ₂ Cl ₂ ^a	K ₂ PtCl ₆ -1	K ₂ PtCl ₆ -2	Iodine	SeMet ^a	Native II
Resolution (Å)	1.8	2.2	2.2	2.2	2.2	2.2	2.4
Space group	P2 ₁ 2 ₁ 2 ₁	P2 ₁ 2 ₁ 2 ₁	P2 ₁ 2 ₁ 2 ₁	P2 ₁ 2 ₁ 2 ₁	P2 ₁ 2 ₁ 2 ₁	P2 ₁ 2 ₁ 2 ₁	C2
R _{merge} (%)	9.9(28.8)	8.2(14.0)	9.4(19.7)	9.0(16.8)	8.5(15.5)	5.0(9.8)	5.7(11.6)
R _{iso} (%)		23.7(25.6)	12.1(19.5)	14.5(18.3)	10.1(14.7)	9.8(11.2)	
No. of sites		2	2	3	1	2	
Phasing power		1.20	1.42	2.79	0.68	1.33	
R _{culis}		0.659	0.534	0.371	0.667	0.717	
Overall FOM to 3.0 Å (centric/acentic)		0.566/0.486					

^a The Pt(NH₄)₂Cl₂ and SeMet data sets were taken on crystals of a K135M mutant, which was isomorphous with Native.

grams from the CCP4 suite (21).

Phasing and Refinement—Five derivatives (Table I) identified via Patterson or cross-difference Fourier were refined using SHARP (22) and solvent-flattened with SOLOMON (21) (the Fe²⁺ and Fe³⁺ derivatives were not used in solving the structure). The isomorphous replacement map was averaged with diffraction data from the unphased C2 crystal form using DMMULTI (21). The model was built with both MIR and averaged maps using O (23). The model was validated with complete omit maps and annealed using CNS (24) with 5% of the reflections reserved for R_{free} statistics. Over the course of phase extension from 3.0 to 1.8 Å, waters were added to the model and checked for chemical sense, and bulk solvent correction was added. Data and refinement statistics are shown in Tables I and II.

RESULTS AND DISCUSSION

Overall Structure of Frataxin—Human frataxin (residues 88–210, lacking the amino-terminal mitochondrial import sequence) is a compact $\alpha\beta$ sandwich (Fig. 2). Elements of secondary structure are labeled in order of sequence (Figs. 1 and 2). Strands β 1– β 5 form a flat antiparallel β sheet that interacts with the two helices, α 1 and α 2. The axes of the two helices are nearly parallel to each other, and both are parallel to the plane of the large β sheet. A second, smaller β sheet is formed by the C terminus of β 5 and strands β 6 and β 7. This smaller sheet projects from the N terminus of α 2 along its long axis. The connections between all elements of secondary structure are short and well ordered, which contributes to the compact appearance of frataxin. Consistent with this appearance, crystallographic temperature factors are low throughout the protein, averaging 23.6 Å² for the entire structure (residues 90–208 and 81 water molecules). A random coil, extending from the C terminus of helix α 2 to the end of the protein, runs antiparallel to the two helices and packs against the body of the protein at the interface between the helices. Search comparisons made using the programs Dali and Cath suggest that the architecture of frataxin represents a new protein fold.

Species Differences—Frataxins from different species are nearly certain to have the same core structures. Elements of secondary structure are conserved (Fig. 1). Consistent with its compact fold, there are no significant insertions or deletions between predicted helices and strands of other frataxins (Fig. 1). However, the frataxin tail sequences, extending from the C terminus of helix α 2, diverge in sequence and differ in length. The 17-residue tail of human frataxin adopts a random coil that is tethered to the body of the domain. Hydrophobic side chains from Leu-198, Leu-200, and Leu-203 of the tail point inward and contribute to the protein core. These residues are undoubtedly necessary for the stability of the mammalian proteins. Most other frataxins, including those from bacteria, have shorter tail sequences with at least two homologous hydrophobic residues. These tail sequences may similarly “cap” the hydrophobic core. However, the yeast homologue Yfh1p has evolved with only four, non-hydrophobic residues C-terminal to helix α 2, suggesting that frataxin tails have no conserved func-

TABLE II
Final model statistics

Resolution	1.8 Å
Reflections	12,425 (1090)
R	19.6 (29.1)%
R _{free}	22.1 (31.5)%
No. water molecules	81
	23.6 Å ²
RMS deviation: bond length/angles	0.0046 Å/1.24°

tion other than protein stabilization.

An Anionic Surface Patch—The clustering of negatively charged residues on one surface of human frataxin is striking (Fig. 3A). Side chains from nine acidic residues project outward from helix α 1: Glu-92, Glu-96, Glu-100, Glu-101, Glu-104, Glu-108, Glu-111, Asp-112, and Asp-115. These are joined by three additional acidic side chains from residues in β 1 at the edge of the large sheet (Glu-121, Asp-122, and Asp-124). The 12 acidic side chains point in the same general direction to form a large, contiguous anionic patch on the protein surface (Fig. 4). The solvent-accessible surface area of the patch is 915 Å², compared with a total accessible surface area for the protein of 4732 Å² (determined using the program CNS (24) and a 1.4-Å probe).

Because few charged groups are distributed over the remaining surface of frataxin, the clustering of acidic residues creates a significant charge dipole. Residues corresponding to human frataxin Glu-100, Glu-108, Glu-111, and Asp-124 are conserved in other animals and in plants, yeast, and eubacteria (Fig. 1). Although other acidic residues within the clusters are less well conserved, because similar numbers of acidic residues are present in the first helix and first strand of all frataxins, all are predicted to have similar anionic surface patches and charge dipoles. Ferritins are iron storage proteins that similarly contain conserved clusters of acidic residues. Twenty-four protomers assemble to form 12-nm hollow spheres, with as many as 4500 iron atoms sequestered in an 8-nm central cavity. Each subunit forms a four-helix bundle. Clusters of acidic residues are required for oxidation of Fe(II) to Fe(III) within channels leading to the core and for ferrihydrite nucleation at the inner surface of the central cavity. Substitutions of individual acidic residues markedly reduce oxidative or nucleation activities (25).

Iron Binding—Because iron accumulates in the mitochondria of cells that lack frataxin activity, it has been postulated that frataxin is involved in iron homeostasis (10, 13). Human frataxin by itself is a monomer, and no iron is present in the bacterially expressed protein, as assessed by atomic absorption (data not shown). We soaked crystals in ferrous sulfate and ferric chloride under conditions similar to those for generating heavy metal derivatives (10 mM for 12 h) to determine whether iron would bind to frataxin. In both cases x-ray diffraction data revealed binding of one iron atom per frataxin molecule, coordinated to His-177. The iron displaces a fixed water molecule and forms a 2.08-Å bond to N^ε of His-177 (Fig. 5). His-177 is in

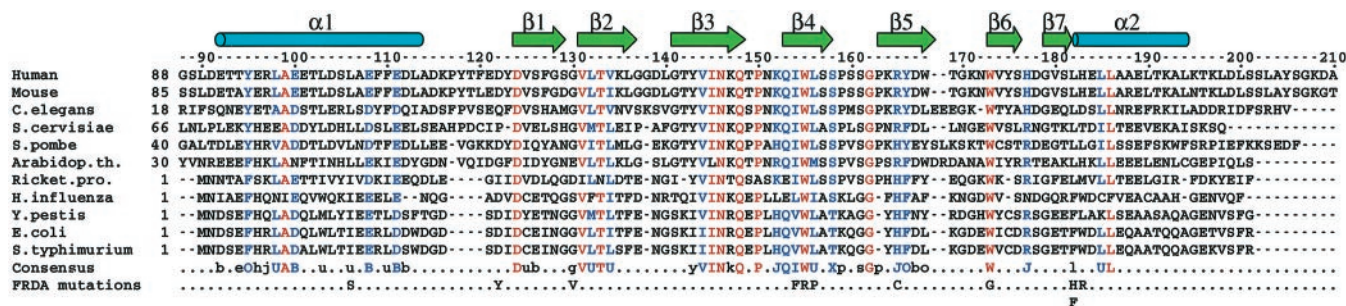


FIG. 1. Structure-based sequence alignment of human frataxin with homologues from prokaryotes and other eukaryotes. Elements of secondary structure are denoted by turquoise cylinders (α helices) and green arrows (β strands). The alignment was by the program Multalin. Identical residues are red. Highly conserved residues are blue. Uppercase residues in the consensus sequence occur with greater than 83% frequency; lowercase residues occur between 67% and 83% frequency. Acidic residues are represented by the letter B (E, D), amides by the letter Z (N, Q), basics by the letter J (R, K, H), aromatics by the letter O (F, Y, W), aliphatics by the letter U (G, A, L, I, V, M), and hydroxyls by the letter X (S, T).

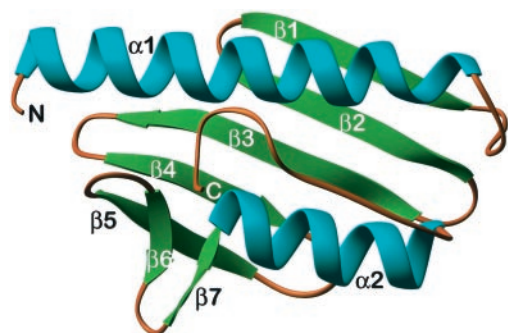


FIG. 2. Structure of frataxin. Ribbon (29) diagrams showing the fold of frataxin, a compact $\alpha\beta$ sandwich, with α helices colored turquoise and β strands in green. Strands $\beta 1$ – $\beta 5$ form a flat antiparallel β sheet that interacts with the two helices, $\alpha 1$ and $\alpha 2$. The two helices are nearly parallel to each other and to the plane of the large β sheet. A second, smaller β sheet is formed by the C terminus of $\beta 5$ and strands $\beta 6$ and $\beta 7$.

the short loop connecting strands $\beta 6$ and $\beta 7$. The His-177 side chain is solvent-exposed, at a site distant from the acidic patch, and lacks interactions with the rest of the molecule. His-177 is at a crystal packing interface, and the iron bound to it is loosely associated ($>4 \text{ \AA}$) with backbone carbonyl oxygens (Ala-114 and Asp-115) and a carboxylate side chain (Asp-115) of an adjacent molecule. For these reasons and most importantly because His-177 is not conserved, the mode of iron binding that we have observed is probably not related to frataxin function in mitochondria. It is more likely that if frataxin binds iron, it does so by assembling with itself or other mitochondrial proteins to utilize its acidic patch as is seen with ferritin (25).

Conserved Outer Surface of the β Sheet—Twenty-six residues in our structure are identical in eukaryotes whose frataxin sequences are currently available, and other residues are highly conserved (Fig. 1). Conserved residues arising from the internal faces of the large sheet and the two helices help form the hydrophobic core of frataxin. An even larger collection of conserved residues forms the external surface of the large β sheet (Fig. 3B). Fifteen residues from strands $\beta 1$ – $\beta 5$ that form this surface are conserved in eukaryotes, and six of these residues are conserved as well in eubacteria. The residues are mostly uncharged, making the flat, 1008-\AA^2 surface nearly neutral. Val-131, Val-144, Pro-150, Trp-155, Pro-159, and Pro-163 add hydrophobicity and potential binding hot spots (26). Residues Thr-133, Thr-142, Asn-146, Gln-148, Asn-151, Gln-153, Ser-161 within this surface, and Asp-124 and Arg-165 at its periphery, render it moderately hydrophilic overall. We predict that this surface might mediate a specific and critical protein-protein interaction, although the putative partner is

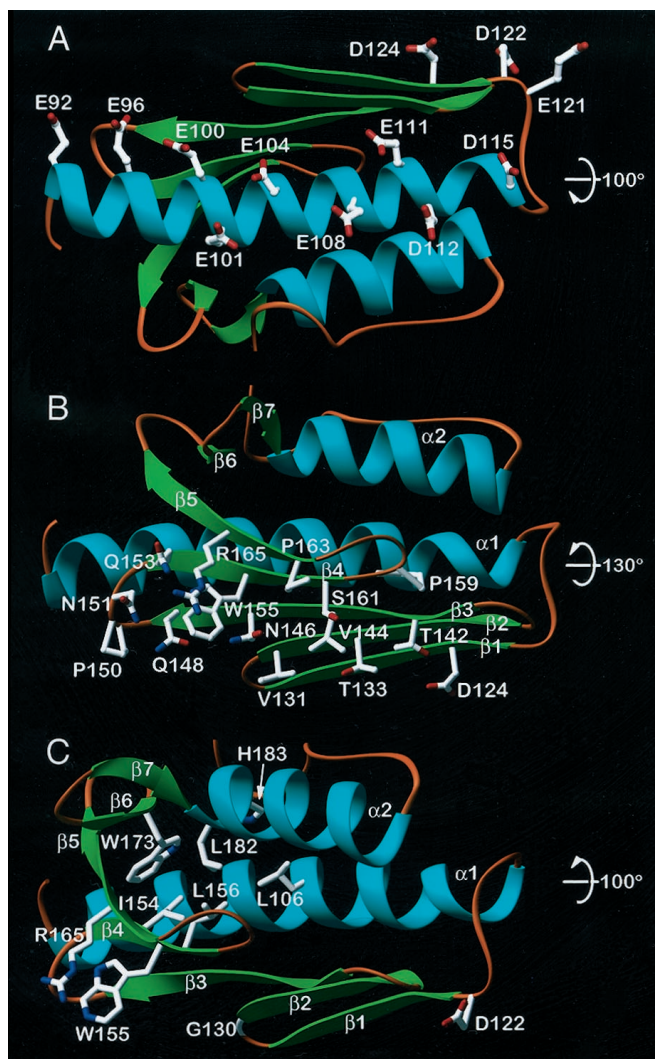


FIG. 3. Specific residues of frataxin and potential functions. A, side chains of 12 acidic residues project from helix $\alpha 1$ and strand $\beta 1$ to create an acidic patch of the surface of the protein. B, side chains of highly conserved residues that project outward from the large, flat β sheet ($\beta 1$ – $\beta 5$) create a 1008-\AA^2 conserved surface on frataxin. C, side chains of residues associated with Friedreich's ataxia point toward the hydrophobic core of frataxin or lie at the periphery of the large β sheet. Structures are rotated the indicated number of degrees about the x axis, relative to the orientation in Fig. 2.

not known. It is hard to imagine why the surface might otherwise be so well conserved.

Mutations Associated with Friedreich's Ataxia—Friedreich's

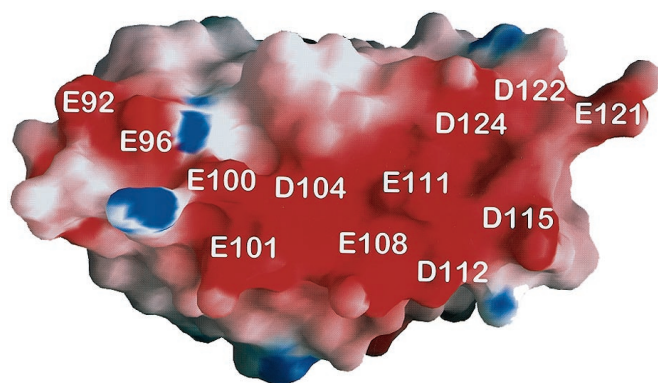


FIG. 4. **Molecular surface representation of frataxin.** The molecule is oriented as shown in Fig. 3A. The molecular surface was calculated and shaded according to the electrostatic potential (-10 *kt/e*, red to $+10$ *kt/e*, blue) using the program GRASP (30). Individual residues within the acidic patch are labeled.

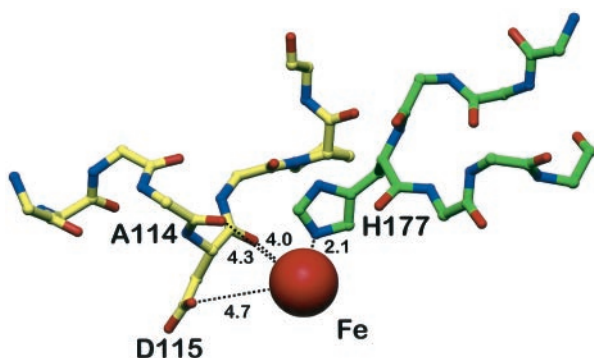


FIG. 5. **Iron binding.** Adjacent frataxin molecules are colored green and yellow. Iron, depicted as a red sphere, is coordinated to His-177. Distances in Å (dotted lines) are between the nucleus of iron and its closest neighbors.

ataxia is caused by abnormalities in both alleles of the *FRDA* locus. Most patients have GAA triplet repeat expansion within intron 1, which leads to abnormally low levels of frataxin protein (5, 6). However, a small percentage of patients are compound heterozygotes having a combination of increased GAA repeats in one allele and a point mutation in the other allele. Thus loss of protein or loss of function similarly cause the disease. Complete loss of function, as occurs with homozygous disruption of the locus in mice, is lethal (27). Known mutations associated with Friedreich's ataxia map to similar sites as the conserved residues (Fig. 3C). Several are in the protein core, including L106S, I154F, L156P, W173G, L182H/L182F, and H183R (7), consistent with a requirement for maintenance of a stable, compact structure. Another mutation, D122Y, is within the anionic patch. This mutation alters charge within this surface and overall protein polarity. The remaining three published mutations, G130V, W155R, and R165C, are located within the flat, conserved external surface of the large β sheet. The fact that mutations within these two conserved surfaces, the anionic patch and the external surface of the β sheet, are

associated with disease firmly supports hypotheses that these surfaces are critical for frataxin function. Patients with D122Y, G130V, and R165C mutations have clinical courses that might be distinguished from other patients (7, 28), indicating that patient phenotypes might be further discriminated on the basis of this structure.

REFERENCES

- Lodi, R., Cooper, J. M., Bradley, J. L., Manners, D., Styles, P., Taylor, D. J., and Schapira, A. H. (1999) *Proc. Natl. Acad. Sci. U. S. A.* **96**, 11492–11495
- Durr, A., Cossee, M., Agid, Y., Campuzano, V., Mignard, C., Penet, C., Mandel, J. L., Brice, A., and Koenig, M. (1996) *N. Engl. J. Med.* **335**, 1169–1175
- Chamberlain, S., Shaw, J., Rowland, A., Wallis, J., South, S., Nakamura, Y., von Gabain, A., Farrall, M., and Williamson, R. (1988) *Nature* **334**, 248–250
- Campuzano, V., Montermini, L., Molto, M. D., Pianese, L., Cossee, M., Cavalcanti, F., Monros, E., Rodius, F., Duclos, F., Monticelli, A., Zara, F., Cañizares, J., Koutnikova, H., Bidichandani, S. I., Gellera, C., Brice, A., Trouillas, P., De Michele, G., Filla, A., De Frutos, R., Palau, F., Patel, P. L., Di Donato, S., Mandel, J.-L., Coccozza, S., Koenig, M., and Pandolfo, M. (1996) *Science* **271**, 1423–1427
- Sakamoto, N., Chastain, P. D., Parniewski, P., Ohshima, K., Pandolfo, M., Griffith, J. D., and Wells, R. D. (1999) *Mol. Cell* **3**, 465–475
- Campuzano, V., Montermini, L., Lutz, Y., Cova, L., Hindelang, C., Jiralerspong, S., Trottier, Y., Kish, S. J., Fauchoux, B., Trouillas, P., Authier, F. J., Durr, A., Mandel, J. L., Vescovi, A., Pandolfo, M., and Koenig, M. (1997) *Hum. Mol. Genet.* **6**, 1771–1780
- Cossee, M., Durr, A., Schmitt, M., Dahl, N., Trouillas, P., Allinson, P., Kostrzewa, M., Nivelon-Chevallier, A., Gustavson, K. H., Kohlschütter, A., Müller, U., Mandel, J. L., Brice, A., Koenig, M., Cavalcanti, F., Tammaro, A., De Michele, G., Filla, A., Coccozza, S., Labuda, M., Montermini, L., Poirier, J., and Pandolfo, M. (1999) *Ann. Neurol.* **45**, 200–206
- Koutnikova, H., Campuzano, V., Foury, F., Dolle, P., Cazzalini, O., and Koenig, M. (1997) *Nat. Genet.* **16**, 345–351
- Wilson, R. B., and Roof, D. M. (1997) *Nat. Genet.* **16**, 352–357
- Babcock, M., de Silva, D., Oaks, R., Davis-Kaplan, S., Jiralerspong, S., Montermini, L., Pandolfo, M., and Kaplan, J. (1997) *Science* **276**, 1709–1712
- Wong, A., Yang, J., Cavadini, P., Gellera, C., Lonnerdal, B., Taroni, F., and Cortopassi, G. (1999) *Hum. Mol. Genet.* **8**, 425–430
- Blass, J. P., Kark, R. A., and Menon, N. K. (1976) *N. Engl. J. Med.* **295**, 62–67
- Rotig, A., de Lonlay, P., Chretien, D., Foury, F., Koenig, M., Sidi, D., Munnich, A., and Rustin, P. (1997) *Nat. Genet.* **17**, 215–217
- Bradley, J. L., Blake, J. C., Chamberlain, S., Thomas, P. K., Cooper, J. M., and Schapira, A. H. (2000) *Hum. Mol. Genet.* **9**, 275–282
- Gray, J. V., and Johnson, K. J. (1997) *Nat. Genet.* **16**, 323–325
- Koutnikova, H., Campuzano, V., and Koenig, M. (1998) *Hum. Mol. Genet.* **7**, 1485–1489
- Gordon, D. M., Shi, Q., Dancis, A., and Pain, D. (1999) *Hum. Mol. Genet.* **8**, 2255–2262
- Knight, S. A., Sepuri, N. B., Pain, D., and Dancis, A. (1998) *J. Biol. Chem.* **273**, 18389–18393
- Branda, S. S., Cavadini, P., Adamec, J., Kalousek, F., Taroni, F., and Isaya, G. (1999) *J. Biol. Chem.* **274**, 22763–22769
- Otwinkowski, T., and Minor, W. (1997) *Methods Enzymol.* **276**, 307–326
- Collaborative Computational Project 4 (1994) *Acta Crystallogr. Sect. D* **50**, 760–776
- LaFortelle, E., Irwin, J. J., and Bricogne, G. (1997) in *Crystallographic Computing* (Bourne, P., and Watenpaugh, K., eds) Oxford Science Publications, Oxford
- Jones, T. A., Zou, J. Y., Cowan, S. W., and Kjeldgaard (1991) *Acta Crystallogr. Sect. A* **47**, 110–119
- Brunger, A. T., Adams, P. D., Clore, G. M., Delano, W. L., Gros, P., Grosse-Kunstleve, R. W., Jiang, J.-S., Kuszewski, J., Nilges, M., Pannu, N. S., Read, R. J., Rice, L. M., Simonson, T., and Warren, G. L. (1998) *Acta Crystallogr. Sect. D* **54**, 905–921
- Chasteen, N. D., and Harrison, P. M. (1999) *J. Struct. Biol.* **126**, 182–194
- Clackson, T., and Wells, J. A. (1995) *Science* **267**, 383–386
- Cossee, M., Puccio, H., Gansmuller, A., Koutnikova, H., Dierich, A., LeMeur, M., Fischbeck, K., Dolle, P., and Koenig, M. (2000) *Hum. Mol. Genet.* **9**, 1219–1226
- De Michele, G., Filla, A., Cavalcanti, F., Tammaro, A., Monticelli, A., Pianese, L., Di Salle, F., Perretti, A., Santoro, L., Caruso, G., and Coccozza, S. (2000) *Neurology* **54**, 496–499
- Carson, M. (1991) *J. Appl. Crystallogr.* **24**, 958–961
- Nicholls, A., Sharp, K. A., and Honig, B. (1991) *Proteins Struct. Funct. Genet.* **11**, 281–296